Supporting Information

Slow internal dynamics and charge expansion in the disordered protein CGRP: a comparison with amylin

Sara M. Sizemore,[§¶] Stephanie M. Cope,[§¶] Anindiya Roy,[‡] Giovanna Ghirlanda[‡] and Sara M. Vaiana[§¶]
[§]Center for Biological Physics, [¶]Department of Physics, [‡]Department of Chemistry and Biochemistry,
Arizona State University, Tempe85287, USA

MATERIALS AND METHODS

Materials. Fmoc(9-fluorenylmethoxycarbonyl)-protected amino acids were purchased from Novabiochem. HOBt (N-hydroxybenzotriazole) and HBTU (O-Benzotriazole-N, N, N', N'-tetramethyl-uronium-hexafluoro-phosphate) were purchased from Genscript. N,N-iisopropylethylamine, or Hünig's base (DIPEA), and N-Methyl-2-pyrrolidone (NMP), used as base in solid phase peptide synthesis, were purchased from Sigma Aldrich. Piperidine (Sigma-Aldrich) was used for deprotection. Rink Amide ChemMatrix® was purchased from Matrix Innovations. Dimethyl formamide (DMF), Dichloromethane (DCM) and Acetonitrile were purchased from Fisher Scientific and were used without further purification.

In addition, >95% purity CGRP wild-type and CGRP D3N mutants, both with the F37W mutation, were purchased from Genscript and purity verified via HPLC on a C18 analytical column. Circular dichroism and TCQ measurements on CGRP F37W purchased from Genscript was identical to measurements on CGRP F37W that was synthesized and purified as described below, and show no difference in secondary or tertiary structure between the two sources.

Peptide synthesis and purification. CGRP F37W was synthesized on a 0.1 mmol scale using a CEM Liberty Automated Microwave Peptide Synthesizer and PALChem Matrix resin. After synthesis, the peptide was thoroughly washed four times by DMF followed by DCM. After washing, the peptide was stored on the resin at -20°C. For deprotection, the peptide was shaken for one hour in 20% piperdine, 0.1M HOBt in DMF and then washed three times. The cleavage cocktail consisted of 81.5% trifluoroacetic acid (TFA) + 5% Water +5% Anisole + 5% Thioanisole + 2.5% 1,2-Ethanedithiol (EDT) + 1% triisopropylsilane (TIS) at the ratio of 150 µL/ 10 mgs of resin. CGRP F37W was purified using Reverse Phase High performance liquid chromatography (HPLC) on a Waters 600E system. Crude peptide was purified on a C4 semi-preparative column (Vydac/Grace Deerfield, IL) from 5-50% Acetonitrile with 0.1% (v/v) TFA at a gradient of 1% every three minutes.

Disulfide formation and oxidized peptide purification. 1.0 mM of lyopholized peptide was dissolved in 30% DMSO and 3% Acetic Acid. The sample was stirred with a magnetic stir bar at 800 rpm. During this time, the formation of the intra-molecular disulfide bonds was monitored via HPLC on a C18 analytical column. The reaction was deemed complete when the reduced peptide's HPLC peak was no longer apparent: approximately 12 hours. After this time, the sample was frozen and lyophilized. Oxidized peptide was re-purified on a C18 semi-preparative column to further purify and separate any un-reacted peptide.

Calibrated MALDI-TOF mass spectrometry indicated the presence of a -2 Da species (above the margin of error the instrument), corresponding to the oxidized form of the peptide. To further support these findings, a maleimide sulfhydryl reaction was performed. 1 mg 3-(N-

Maleimidopropionyl)-biocytin (Cayman Chemical Company Ann Arbor, MI) was dissolved in 180uL 20mM PBS buffer, pH=7.0 and 20μL acetonitrile. Approximately 0.1mg pure, oxidized CGRP F37W was dissolved in 90μL 20mM PBS buffer, pH=7.0 and 10μL acetonitrile, and 50 μL of this solution was combined with the 3-(N-Maleimidopropionyl)-biocytin solution and shaken for four hours. At 1 hour increments, 50 μL aliquots were removed and frozen in dry ice. After four hours, the four aliquots were analyzed via MALDI-TOF MS.

HPLC peaks were analyzed by a Voyager Systems 4320 (Applied Biosystems) matrix assisted laser desorption/ionization-time of flight mass spectrometer (MALDI-TOF MS). The peak corresponding to a molecular weight of 3828Da (corresponding to the amidated and oxidized form of CGRP F37W) was analyzed further for purity by analytical HPLC, using a reverse phase C18 analytical column 214TP54 (Length 250mm × ID 4.6mm) particle size 5μm using the same gradient conditions with 0.9 mL/min flow rate. A single peak eluting at a gradient corresponding to the hydrophobicity of CGRP was collected, immediately frozen in liquid nitrogen, lyophilized, and kept at -20°C.

Circular dichroism measurements. CD Spectra of the samples were measured in 1mm quartz cuvettes (Starna Cells). Aliquots of solutions prepared for TCQ were diluted with Millipore H_2O, resulting in final peptide concentrations ranging from 10-40 μM. A Jasco J-710 spectropolarimeter (Jasco Company) was used with a 1 nm bandwidth. For each sample, eight spectra taken with a 0.2 nm pitch at a 50 nm/min scan speed were averaged. Before data analysis, spectra were buffer subtracted.

Salt dependence of k_{obs} and k_R for CGRP. In the discussion of Figure 5 (salt dependence of k_{obs} for D3N CGRP at pH 3), it is assumed that $k_{obs} \approx k_R$, so that any variation in k_{obs} directly reflects a variation in the end-to-end distance distribution rather than in the diffusional dynamics. To test this, we measured the viscosity and temperature dependence of k_{obs} at two extreme salt concentrations, 0M and 500mM KCl (Figure S3 bottom two panels) and directly compared the values of k_R with those of k_{obs}. The values of k_R, obtained from the global fit results of Figure S3 (as described in Methods) are shown in the table below. We find that the values measured under the two extreme salt concentrations remain proportional, with a proportionality constant A given by:

$$A = \frac{k_{obs}}{k_R} \qquad (1)$$

Rate	0M KCl	500mM KCl
k_{obs}	0.30 ± 0.03 μs^{-1}	0.63 ± 0.06 μs^{-1}
k_R	0.43 ± 0.04 μs^{-1}	0.88 ± 0.09 μs^{-1}
A	0.708 ± 0.097	0.717 ± 0.100

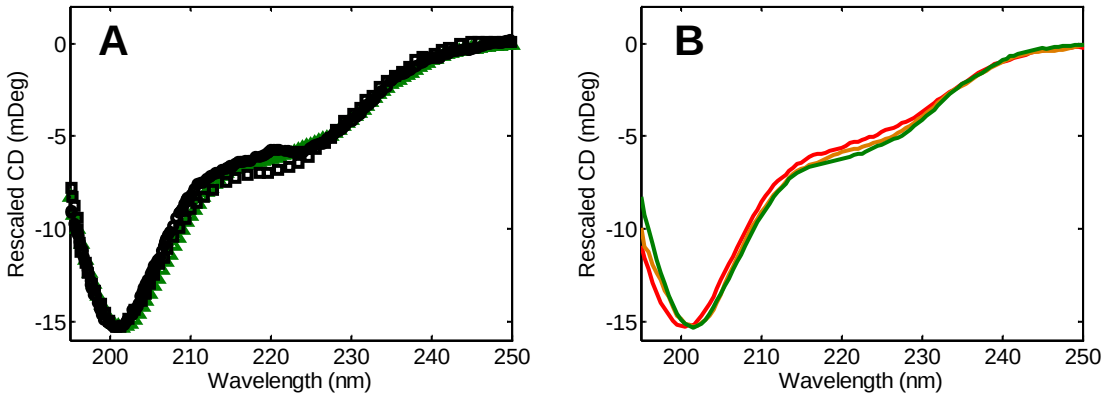

Figure S1: **(A)** Far-UV CD spectra of CGRP F37W at pH 8 at 20C (green triangles) compared to previously published data for CGRP wild-type by *Oconnell et al.* (Oconnell, J. P.; Kelly, S. M.; Raleigh, D. P.; Hubbard, J. A. M.; Price, N. C.; Dobson, C. M.; Smith, B. J. *Biochemical Journal* **1993**, *291*, 205) (open black circles) and by *Manning et al.* (Manning, M. C. *Biochemical and Biophysical Research Communications* **1989**, *160*, 388) (open black squares), rescaled by the signal at the minimum at 20C. The F37W mutation does not affect the secondary structure of CGRP. **(B)** Far-UV CD spectra of CGRP F37W at pH 3 (red), 4.9 (orange) and 8 (green) at 20C, normalized by the minima at 200 nm. No significant variation in secondary structure content as a function of pH is apparent, confirming previous far-UV CD measurements of wtCGRP in the same pH range(Hubbard, J. A. M.; Martin, S. R.; Chaplin, L. C.; Bose, C.; Kelly, S. M.; Price, N. C. *Biochemical Journal* **1991**, *275*, 785).

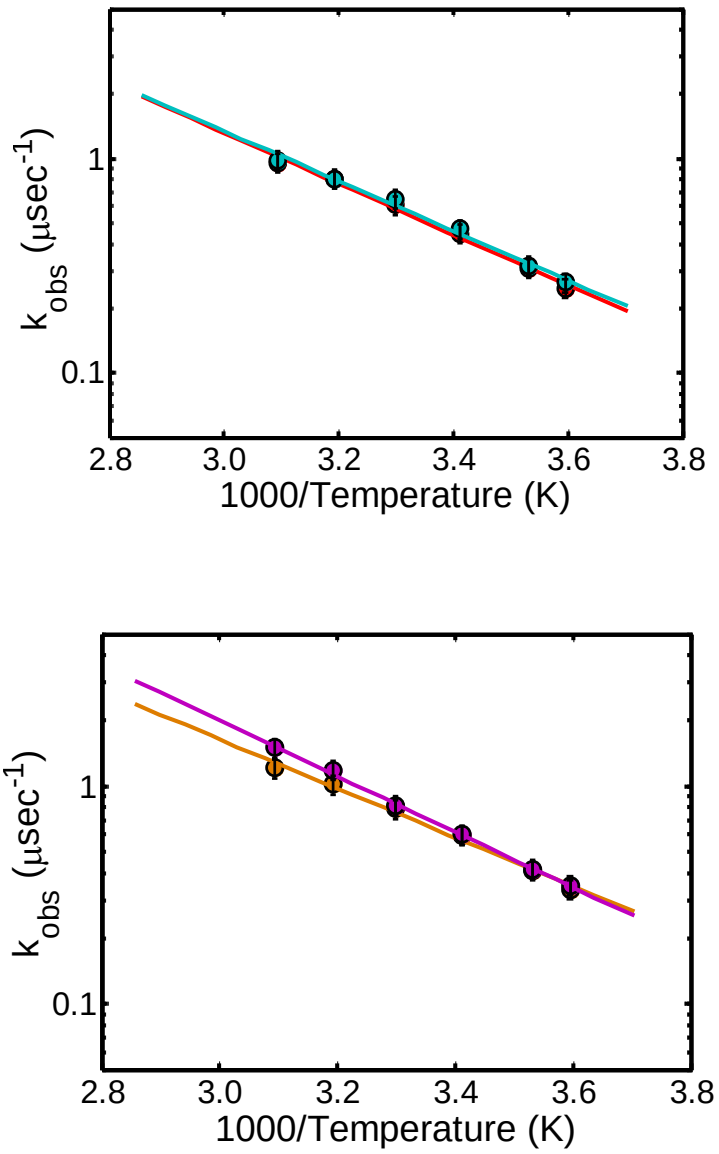

Figure S2: *Top:* Comparison of k_{obs} measured for D3N CGRP at pH 4.9 (cyan) and wt CGRP at pH 3 (red) corresponding to a peptide net charge of roughly +6 in both cases. The values of k_{obs}measured at both pH values are virtually indistinguishable. This confirms that the difference in k_{obs} measured for CGRP at pH 4.9 versus pH 3 (Figure 4 main text) is due to the loss of charge on the aspartic acid and not to other possible direct effects of pH. *Bottom:* comparison of k_{obs} for D3N CGRP at pH 8 (magenta) with wt CGRP at pH 4.9 (orange), both corresponding to a peptide net charge of about +5.

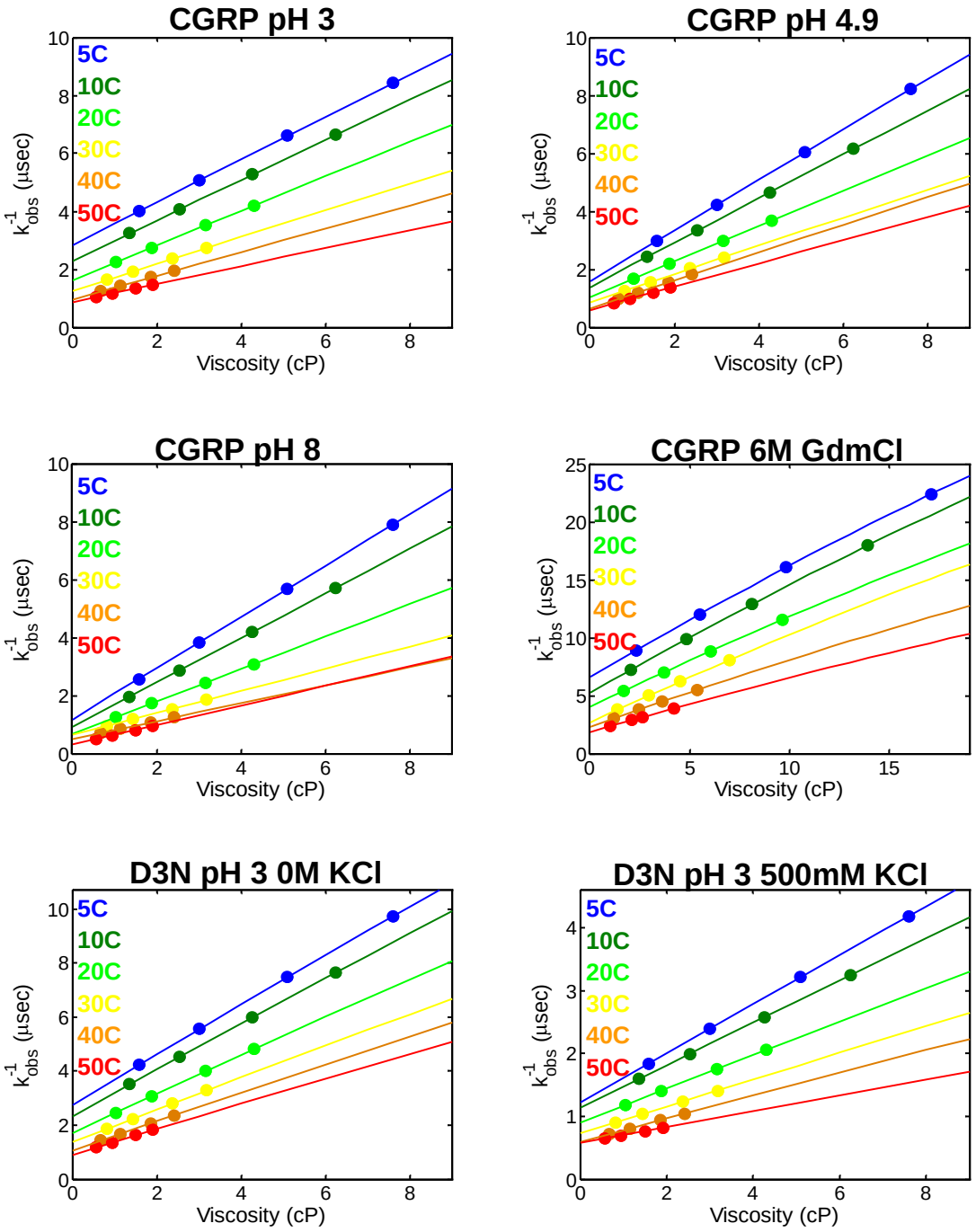

Figure S3: Results from global fits of the tryptophan triplet state decay curves (Figure 2 main text), at different temperatures and solvent viscosities, as described in Methods. Values of k_{obs}^{-1} obtained from global fits are plotted as a function of the solvent viscosity at each temperature. The reaction limited rate $k_R(T)$, is obtained from the y-intercept at each temperature, the diffusion limited rate k_{D+} from the slope at each temperature, as described in Methods (main text). For each peptide/solution condition a set of about 120 decay curves were used for the global fitting.

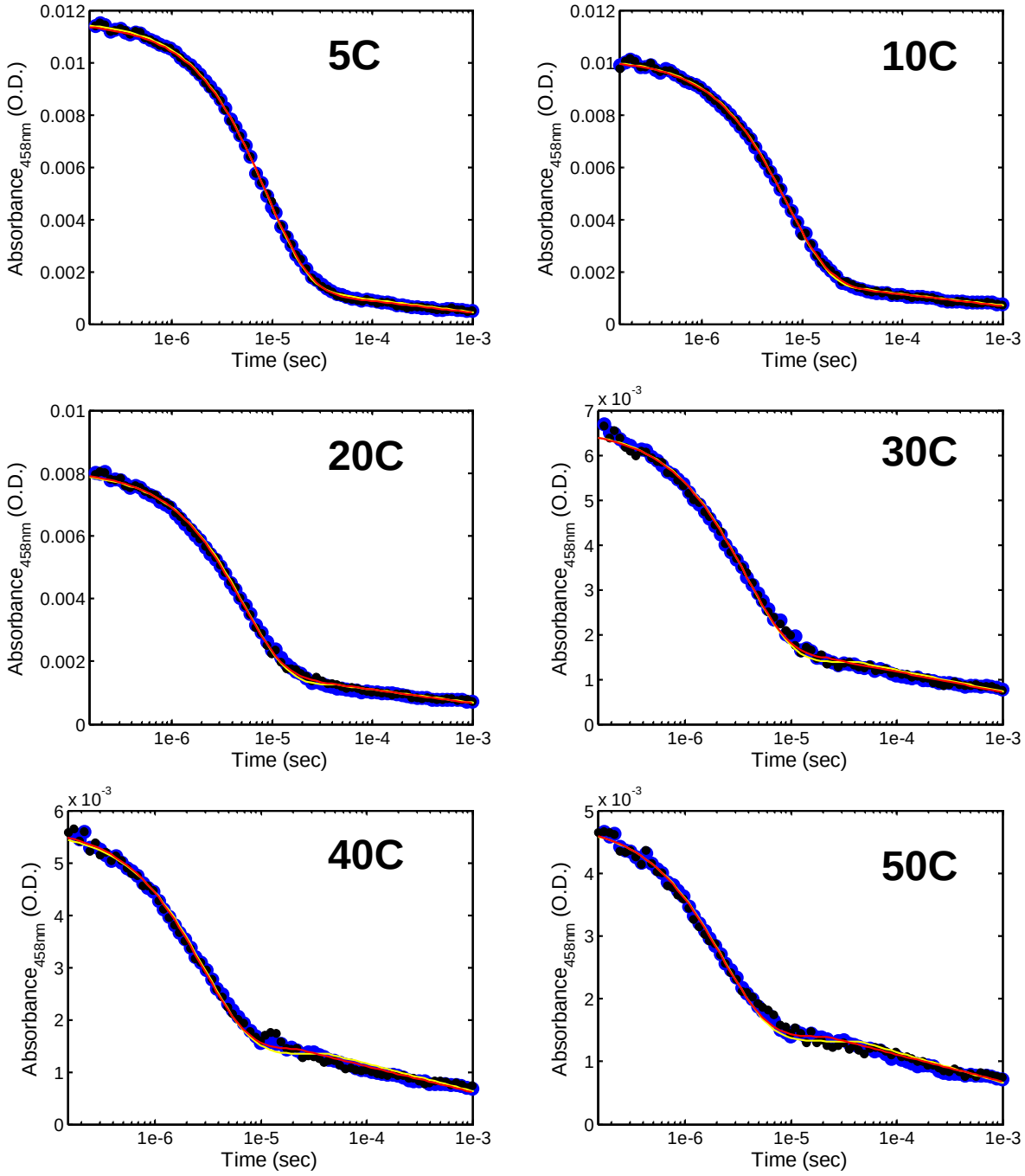

Figure S4: Tryptophan triplet state decay curves of *wt* CGRP at different temperatures in 6 M GdmCl, measured from the decay of tryptophan triplet-triplet absorption after nanosecond excitation. *Black circles*: data obtained from directly averaging all traces at each temperature; *blue circles:* data obtained after noise reduction by singular values decomposition (SVD), as described in the main text (data of Figure 2); *yellow lines:* best fit curves obtained by globally fitting the noise reduced data (blue points), as described in the main text (lines of Figure 2); *red*

lines: best fit curves obtained by directly fitting the average data at each temperature (black circles) individually.

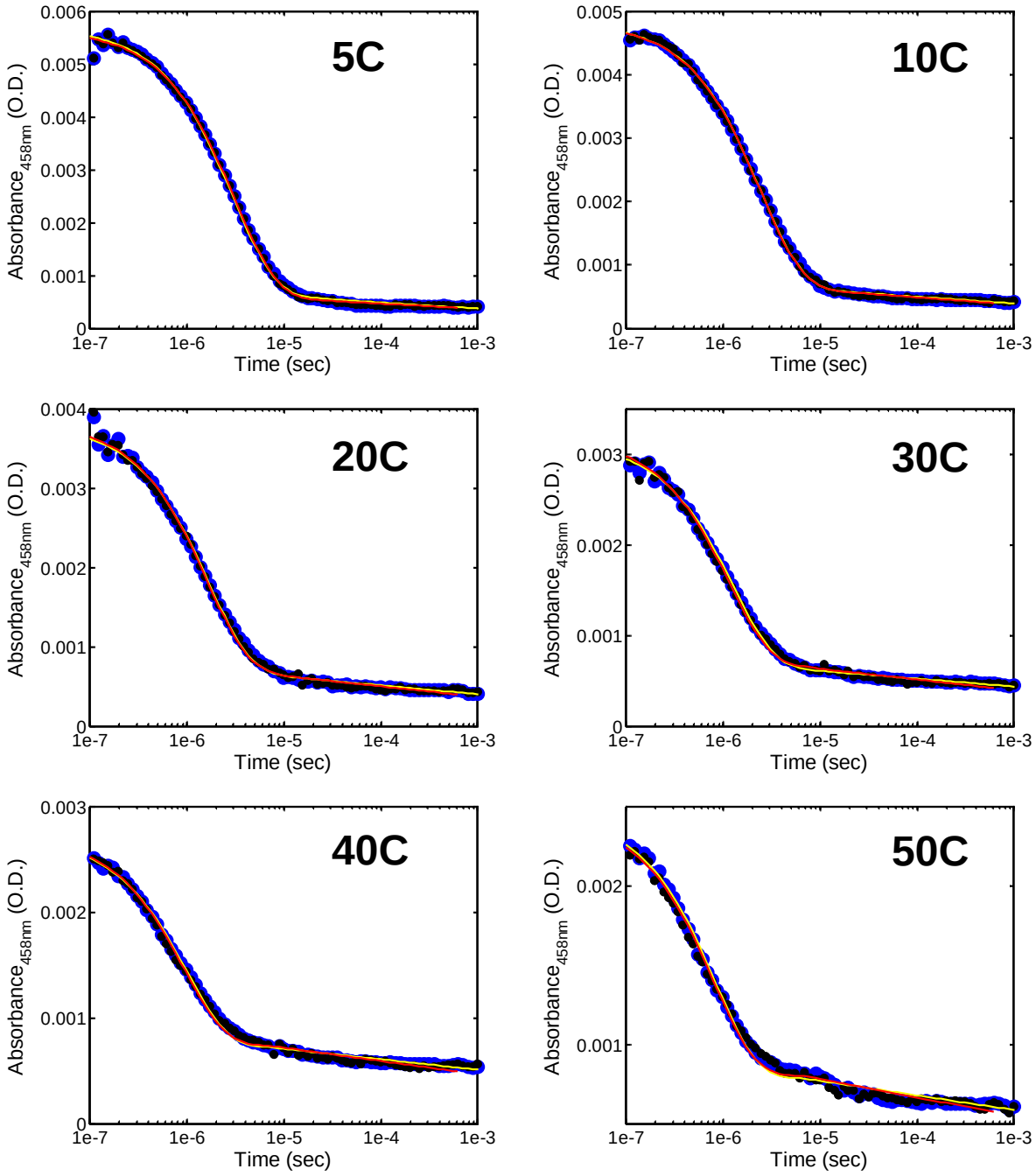

Figure S5: Tryptophan triplet state decay curves of *wt* CGRP at different temperatures in buffer at pH 4.9, measured from the decay of tryptophan triplet-triplet absorption after nanosecond excitation. *Black circles*: data obtained from directly averaging all traces at each temperature; *blue circles:* traces obtained after noise reduction by singular values decomposition (SVD), as described in the main text (data of Figure 2); *yellow lines:* best fit curves obtained by globally

fitting the noise reduced data (blue points), as described in the main text (lines of Figure 2); *red lines:* best fit curves obtained by fitting the average data at each temperature (black circles) individually.

	SVD Global Fit (μs^{-1})		Individual Fit (μs^{-1})		Percent Difference	
Temperature	**6M GdmCl**	**pH 4.9**	**6M GdmCl**	**pH 4.9**	**6M GdmCl**	**pH 4.9**
5C	0.11 (0.12)	0.34 (0.35)	0.11 (0.12)	0.32 (0.35)	0.2% (-1.3%)	4.8% (1.3%)
10C	0.14 (0.14)	0.41 (0.41)	0.14 (0.14)	0.41 (0.41)	-2.0% (-2.0%)	-0.5% (0.1%)
20C	0.19 (0.19)	0.59 (0.57)	0.20 (0.19)	0.62 (0.58)	-6.2% (-3.4%)	-3.5% (-2.1%)
30C	0.26 (0.25)	0.79 (0.76)	0.27 (0.26)	0.87 (0.79)	-2.9% (-4.7%)	-10.3% (-4.3%)
40C	0.33 (0.33)	1.02 (1.00)	0.36 (0.35)	1.08 (1.06)	-8.1% (-5.9%)	-6.2% (-6.3%)
50C	0.42 (0.43)	1.21 (1.29)	0.44 (0.46)	1.26 (1.39)	-5.3% (-7.1%)	-4.3% (-8.3%)

Table S1: Comparison between the values of k_{obs} for wt CGRP (in units of inverse microseconds) obtained using two alternative methods of Figures S4 and S5: *i)* globally fitting the noise reduced SVD traces as described in the main text and used throughout the paper (these are best fit values corresponding to the yellow lines of Figures S4 and S5); *ii)* individually fitting each average trace at a given temperature. The numbers in parenthesis are the theoretical values obtained from a simple Arrhenius temperature fit of k_{obs} versus T and correspond to the straight lines of Figure 3 and 4 (these values at 20C are reported in Table 1).